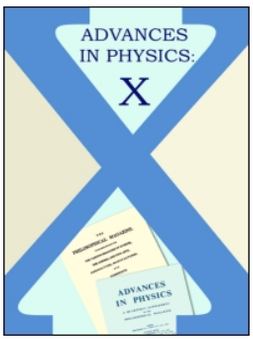

Advances in Physics: X

ISSN: (Print) 2374-6149 (Online) Journal homepage: https://www.tandfonline.com/loi/tapx20

# Invariance of parameter identification in multiscales of meta-atoms in metamaterials

Osamu Sakai, Akinori Iwai & Yoshiharu Omura

**To cite this article:** Osamu Sakai, Akinori Iwai & Yoshiharu Omura (2018) Invariance of parameter identification in multiscales of meta-atoms in metamaterials, Advances in Physics: X, 3:1, 1433551, DOI: 10.1080/23746149.2018.1433551

**To link to this article:** https://doi.org/10.1080/23746149.2018.1433551



Published online: 15 Feb 2018.

ADVANCES IN PHYSICS: X
2018, VOL. 3, NO. 1, 1433551
https://doi.org/10.1080/23746149.2018.1433551

Taylor & Francis
Taylor & Francis Group

REVIEW ARTICLE

OPEN ACCESS Check for updates

# Invariance of parameter identification in multiscales of meta-atoms in metamaterials

Osamu Sakai[a], Akinori Iwai[b] and Yoshiharu Omura[b]

[a]Electronic Systems Engineering, The University of Shiga Prefecture, Hikone, Japan; [b]Research Institute for Sustainable Humanosphere, Kyoto University, Uji, Japan

**ABSTRACT**

The concept of metamaterials has led to extraordinary schemes of wave propagation, which has been verified using various meta-atoms, constituent units of metamaterials, as well as applied to a number of categories in physics. Although its definition clarifies the maximum size of meta-atoms as a fraction of one wavelength, the size may vary by several orders, like from millimeters ('macroscopic level') to atomic scales ('microscopic level') for microwaves. This review surveys several patterns of parameter combinations, like permittivity and permeability in electromagnetic metamaterials, which have been achieved at either macroscopic or microscopic levels, with the similar analogy under the concept of metamaterials. Various experimental and theoretical efforts reported so far and shown here verify that the parameter identification of these values (permittivity, permeability, and refractive index) is independent of meta-atom sizes, with importance of spatial integration procedure on the order of a wavelength.

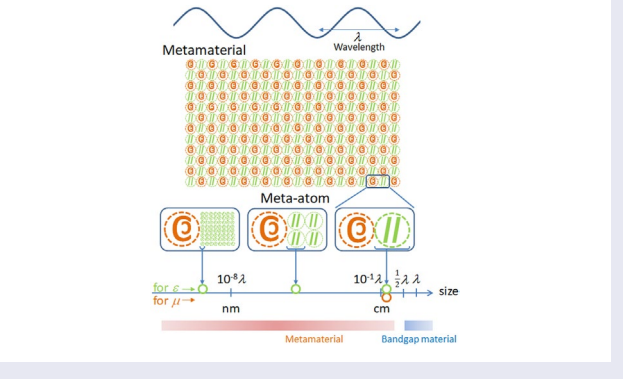


**ARTICLE HISTORY**
Received 18 November 2017
Accepted 3 January 2018

**KEYWORDS**
Wave; metamaterial; plasma; permittivity; permeability; refractive index

**PACS**
41.20.Jb Electromagnetic wave propagation; radiowave propagation; 52.35.Hr Electromagnetic waves; 78.20.Ci Optical constants; 77.22.Ch Permittivity (dielectric function)

**CONTACT** Osamu Sakai sakai.o@e.usp.ac.jp

## 1. Introduction

Metamaterials are fascinating materials as wave media since their performances include parameters with extraordinary values in the media [1–8]. They have designable microstructures whose sizes are much less than the wavelength of a given wave, and the careful design and subsequent fabrication bring us various abnormal scientific features and advanced technological merits simultaneously. One of the features that naturally available solid materials cannot achieve but metamaterials can possess is the negative sign in permittivity $\varepsilon$ [9,10] and/or permeability $\mu$ [11,12]. The proposal for negative $\mu$ was initially performed using an array of double split ring resonators (DSRRs) [11], and it is successful in a number of experiments. In such studies, the typical size of an individual unit like a DSRR, hereafter referred to as a *meta-atom*, has about 1/5–1/10 of the wavelength of electromagnetic waves tested in experiments; DSRRs actually fit to the definition of metamaterials. Negative $\varepsilon$ was also achieved using metamaterials, whose configurations usually take the forms of a metallic-pole array (or cut wires) [9] or a perforated metallic plate [13]. Schematic examples of metamaterial structures with a given wavelength are shown in Figure 1

When we take a closer look at a metamaterial, we recognize inhomogeneous field profiles depending on its microscopic structure. Numerical results obtained by a numerical simulator reveal that calculated distributions of electric fields $E$ are fairly inhomogeneous with fine structures whose characteristic lengths are much less than those of propagating waves [6]. We confirmed similar patterns in emissions of plasma generated on a DSRR at relatively high gas pressure (Ar at 5 kPa) as shown in Figure 2 [14], which also indicates that $E$ is localized not as a propagating field but a component similar to that around an equivalent lumped circuit element. Consequently, the magnetic fields $H$ include a similar inhomogeneous distribution according to electromagnetic theory. The extraordinary parameters like negative values in $\varepsilon$ and $\mu$ arise from integration or mathematical integral treatment of such fine field structures over one wavelength.

In an electromagnetic metamaterial, since an electromagnetic wave has two kinds of fields, $E$ and $H$, refractive index $N$ is given as [2,6,12,14].

$$N = \sqrt{\varepsilon}\,\sqrt{\mu}. \tag{1}$$

That is, synthesis effects of $\varepsilon$ and $\mu$ are essential on $N$. In a naturally available homogeneous material, this synthesis process is continuous due to simultaneous mixing of electric and magnetic flux densities $D$ and $B$ with $E$ and $H$ during propagation of an electromagnetic wave; $\varepsilon$ and $\mu$ are given by the following formulae: $D = \varepsilon\varepsilon_0 E$ and $B = \mu\mu_0 H$, where $\mu_0$ and $\varepsilon_0$ are the permeability and the permittivity in vacuum, respectively. Thus far, parameter retrievals for $\varepsilon$, $\mu$ and $N$ have been established [15,16], and equal spatial periodicity of meta-atoms for $\varepsilon$ and $\mu$ is typical in cases of metamaterial experiments.

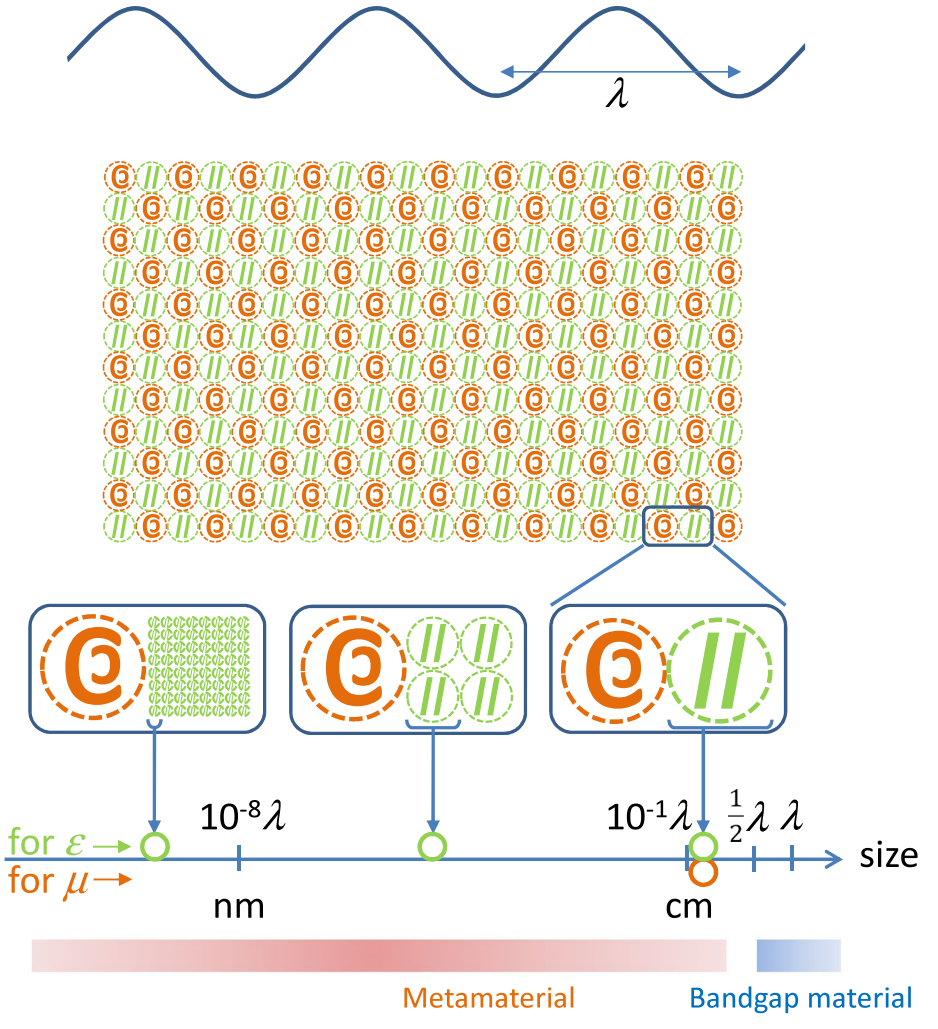


**Figure 1.** Schematic view of metamaterial configuration with various sizes of unit microstructure.

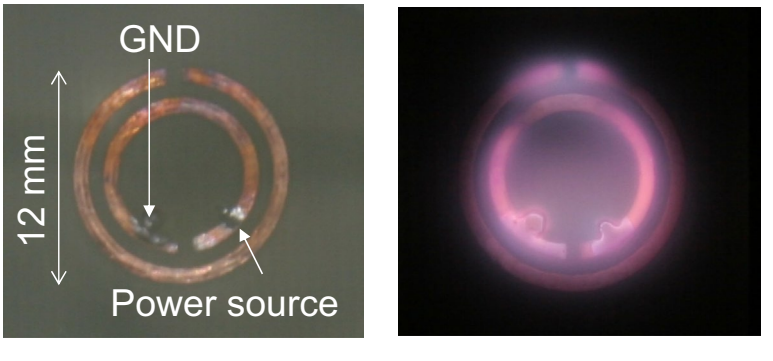


**Figure 2.** Visible emissions, Ref. [14], from DSRR when discharge voltage is applied. Emission pattern is very similar to that of local electric fields which are numerically calculated [6].

On the other hand, as we stated above, the field distributions are fairly inhomogeneous in metamaterials, and we have to confirm the validity of synthesis or collaboration effects between $\varepsilon$ and $\mu$ for $N$, even in cases where the meta-atom sizes for controls of $\varepsilon$ and $\mu$ are different. There exist wave constituents that belong to near fields and propagating modes, either of which fulfills the Maxwell equations, and the propagating modes mainly determine metamaterial outputs, while all fields subject to both constituents will be integrated to estimate macroscopic $\varepsilon$ and $\mu$ over a sufficient size. $\varepsilon$ and $\mu$ can be separately treated in a different size of the meta-atoms, and their sizes might be different. One possible manner is requirement of synchronous distributions between $E$ and $H$ in microscopic profiles per unit. Another possible manner is synthesis of $\varepsilon$ and $\mu$ after each identification from independent contributions of two metamaterial components over one wavelength. A visual representation is displayed in Figure 1; good matching of $E$ and $H$ with the same size or spatial periodicity was in almost all cases of the metamaterials previously reported. However, one of them (e.g. the meta-atom for $\varepsilon$ in Figure 1) might be much smaller than the other.

Another and somewhat conclusive description about size issues of metamaterials is restriction within the Bloch modes. When a microstructure with the unit length $a$ is spatially periodic in an infinite space, a temporal vector field $A(x,t)$ at time $t$ at a specific position $x$ is $A(x+a,t) = A(x,t)\exp(jka)$ [14,17], where $k$ is the wavenumber along the $x$ axis, and this mathematical relation leads to the corresponding dispersion relation. Note that $A(x,t)$ includes both near fields and propagating modes. This unit size gives us maximum of $k$ as $\pi/a$.

Then, the points we have to settle here are the following: (1) $N$ given by Equation (1) with suitable identifications of $\varepsilon$ and $\mu$, and (2) effects of spatial periodic length of meta-atoms in metamaterials $a$ on forming of $N$.

In this study, we review identifications of parameters in metamaterials, and examine such synthesis effects in metamaterials using various experimental and numerical results. In addition to electromagnetic metamaterials, acoustic metamaterials are also surveyed about their meta-atom sizes in comparison with wavelengths. In particular, our main interest is in plasma-metamaterial composites [14], in which the unit sizes of metamaterials for $\varepsilon$ and $\mu$ are different by several orders, and the synthesis is successful for achievement of negative $N$. Finally, we discuss the manner of synthesis between $\varepsilon$ and $\mu$ for $N$ using various configurations in a one-dimensional (1D) numerical model.

## 2. Survey of previous accomplishments of negative refractive index

To generalize underlying principles for pursuing synthesis in $N$, we carry out our data acquisition from two categories of metamaterials: electromagnetic metamaterials and acoustic metamaterials. In an electromagnetic metamaterial [2–5,7], electromagnetic waves propagate according to the following wave equation [6,14]:

$$\nabla \times (\nabla \times \boldsymbol{E}) = -\mu\mu_0 \frac{\partial}{\partial t}\left(\varepsilon_0 \frac{\partial \boldsymbol{E}}{\partial t} + \boldsymbol{J}\right) \equiv -\frac{\varepsilon\mu}{c}\frac{\partial^2 \boldsymbol{E}}{\partial t^2}, \tag{2}$$

where $t$ is time, $\boldsymbol{J}$ the external current density, and $c$ the velocity of light. The contribution of $N^2$ is in the last term of Equation (2). $\boldsymbol{J}$ is significant when we consider presence of plasma [14]. One of the typical meta-atoms for negative $\mu$ is a DSRR, and its size almost covers the periodic length of meta-atoms in metamaterials. The meta-atom for negative $\varepsilon$ is, for instance, a metal strip line [9], and its width is quite small, while the length of one unit should be measured using a periodic length of the meta-atom.

In cases of acoustic metamaterials [8,18–22], propagating acoustic waves are given as [8,19].

$$(\nabla \cdot \nabla)P - \frac{\rho}{M}\frac{\partial^2 P}{\partial t^2} = 0, \tag{3}$$

where $P$ is pressure. That is, to control $N$ in acoustic metamaterials, bulk modulus $M$ (or $1/M$ in comparison with $\varepsilon\varepsilon_0$) and mass density $\rho$ (in comparison with $\mu\mu_0$) are constituents of the product that form $N$. One of the typical meta-atom examples for negative $M$ is a side hole that is configured on the side of a flow path of acoustic waves, and that for negative $\rho$ is a membrane that is installed at a position against the waves [8]. Their sizes are much smaller than the corresponding wavelength, and here we re-measure the sizes as their periodic length in the metamaterial structure.

Our survey, which covers both electromagnetic and acoustic metamaterials, is about size of meta-atoms in comparison with wavelength. Here, we limit its maximum size as a half wavelength since the lowest bandgap forms at the half wavelength, and the higher-order bandgaps exist in the larger-size range.

Figure 3 shows a chart for various previously reported studies [18,23–28] with data points of size/wavelength ratio as a function of wavelength. This survey covers a variety of working frequencies and also both categories of electromagnetism and acoustics, and all of the studies showed achievements of negative $N$. In all cases, the sizes of the unit meta-atoms ranges from 1/5 to 1/50, and all of them have spatially synchronous structures that have the same length of two meta-atoms for $N$. One unique study is in Ref. [28], where no artificially designed spatial periodicity was found, indicating that size of meta-atoms has less limitation of regulations. A further exceptional case is a plasma-metamaterial composite, which will be described in the following sections.

## 3. Experimental results on plasma-metamaterial composites

In this section, we demonstrate the previous studies about electromagnetic metamaterials composed of plasma [14,29–32], in which various sizes of meta-atoms

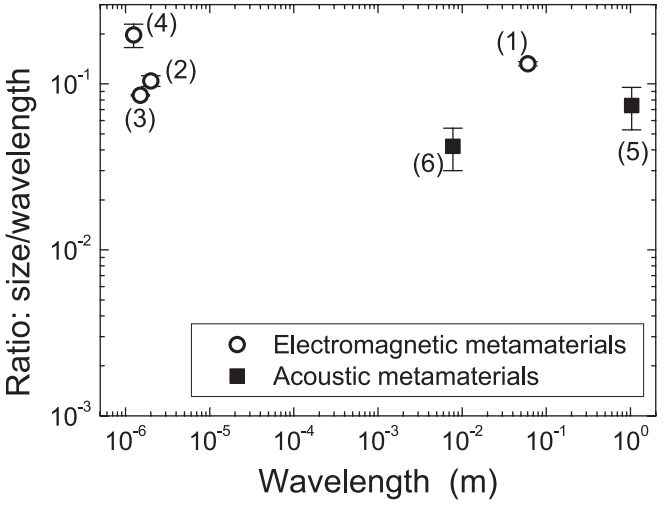


**Figure 3.** Ratio between size and wavelength as a function of wavelength in various electromagnetic and acoustic metamaterials. Data are derived from: (1) [24], (2) [25], (3) [26], (4) [27], (5) [18], and (6) [28].

in metamaterials work to exhibit extraordinary $N$. Plasma is not always a unique medium that has a variety of sizes of microstructures, but it is still typical and suitable to discuss several effects on $N$ since we can measure $\varepsilon$ directly, which gives us straightforward evidence for the phenomena. Information of electron density $n_e$, whose values in plasma can be measured using various methods, provides us a value of $\varepsilon$ since oscillations of free electrons with $n_e$ determine $\varepsilon$ by the well-known formula, given as [14].

$$\varepsilon = 1 - \frac{\omega_{pe}^2}{\omega^2} = 1 - \frac{e^2 n_e}{\varepsilon_0 m_e \omega^2}, \tag{4}$$

where $\omega_{pe}$ is the electron plasma frequency, $\omega$ the angular wave frequency, $e$ the elementary charge, $\varepsilon_0$ the permittivity in vacuum, and $m_e$ the mass of an electron. Here, we assume that electron elastic collision frequency is negligible in comparison with $\omega$, and such experimental parameters are easily available and controllable in experiments unlike $\varepsilon$ of metals in a photon range, which is also in the similar Drude model [33].

Plasma-metamaterial composites in which $\varepsilon$ in Equation (4) is effective were reported on findings and verifications of negative $N$ in several experiments, and here we review them [14,29–32], and discuss the common and different scientific points in comparison with solid-state metamaterials. When we make $\mu$ negative in a given space by solid-state metamaterials, $\varepsilon$ is positive before plasma generation or when $n_e$ is fairly low, leading to imaginary $N$ and electromagnetic waves being evanescent. As $n_e$ increases, beyond the value where $\varepsilon$ is zero, plasma becomes *overdense* and $\varepsilon$ becomes negative. Thus, $N$ becomes real and negative, and the

waves can propagate in the plasma-metamaterial composite. Note that $N$ for propagation modes is limited to the maximum value since the metamaterial induces spatial periodicity [14,17].

### 3.1. Case of synchronization of discrete periodic microstructures

When we use microplasmas whose sizes range from μm to mm [34,35], relative size of the meta-atom composed of plasma-filled space is controllable with respect to a wavelength of a given electromagnetic wave.

The setup of experiments in which microplasmas work to create negative $\varepsilon$ is shown in Figure 4(a) [14,29]. On a coplanar waveguide, an array of double metallic helices was installed, and a dielectric layer covered each metallic wire. It was expected to work as a negative-$\mu$ metamaterial, although the negative value was not solely confirmed since this structure works by coupling to the metallic plates of the coplanar waveguide [29,36]. The metallic components in the helix were almost perpendicular to $E$ in the coplanar waveguide, and the effects on $\varepsilon$ were negligible [36]. Beside its function as a negative-$\mu$ material, it also worked as a discharge electrode on which low-frequency high voltage was applied. Generated microplasmas, which were expected to work as a negative-$\varepsilon$ material, penetrate and surround these helical structures in the shape of columns, and both materials were perfectly synchronized with their locations. The state of negative $\varepsilon$ by microplasmas was confirmed by an indirect measurement of $n_e$ based on density detection of metastable He atoms [29]. The total configuration was a compact system, and estimated as a device under test (DUT) using low-power microwaves that propagate in the linear regime with no effects on $n_e$.

Figure 4(b) shows a dynamic change in phase of a transmitted wave through DUT during the time period of decreasing $n_e$ in microplasmas [14,29]. At most frequencies it shows a slight change, but its change was very large around a specific frequency (4.297 GHz, ~ resonance frequency) when microplasmas were in the afterglow. This is attributed to significant contribution of negative-$\mu$ material, which has a negative value at a limited frequency band since $\mu$ changes significantly near the magnetic resonance frequency due to an inductance-capacitance resonance in the equivalent circuit of the metallic helices [36]. The negative state of $\mu$ was not confirmed experimentally, but synthesis effects of microplasma generation and magnetic resonance were quite clear; otherwise, without either of them, the phase change was limited to a small value. Estimated values of $N$ from the analytical method for layered microwave planar waveguides [37] is within the range ($|N| < 14$) restricted from the maximum $k$ ($=\pi/a$) in the Bloch mode.

This experiment confirms the validity of plasma as a negative-$\varepsilon$ material and good synthesis as a metamaterial effect composed of multiple components. In fact, similar effects arising from electron oscillations in metals lead to negative $\varepsilon$ in optical negative-index metamaterials [19]; an array of metal rods, with shapes quite similar to our microplasma columns, can make $\varepsilon$ negative [5].

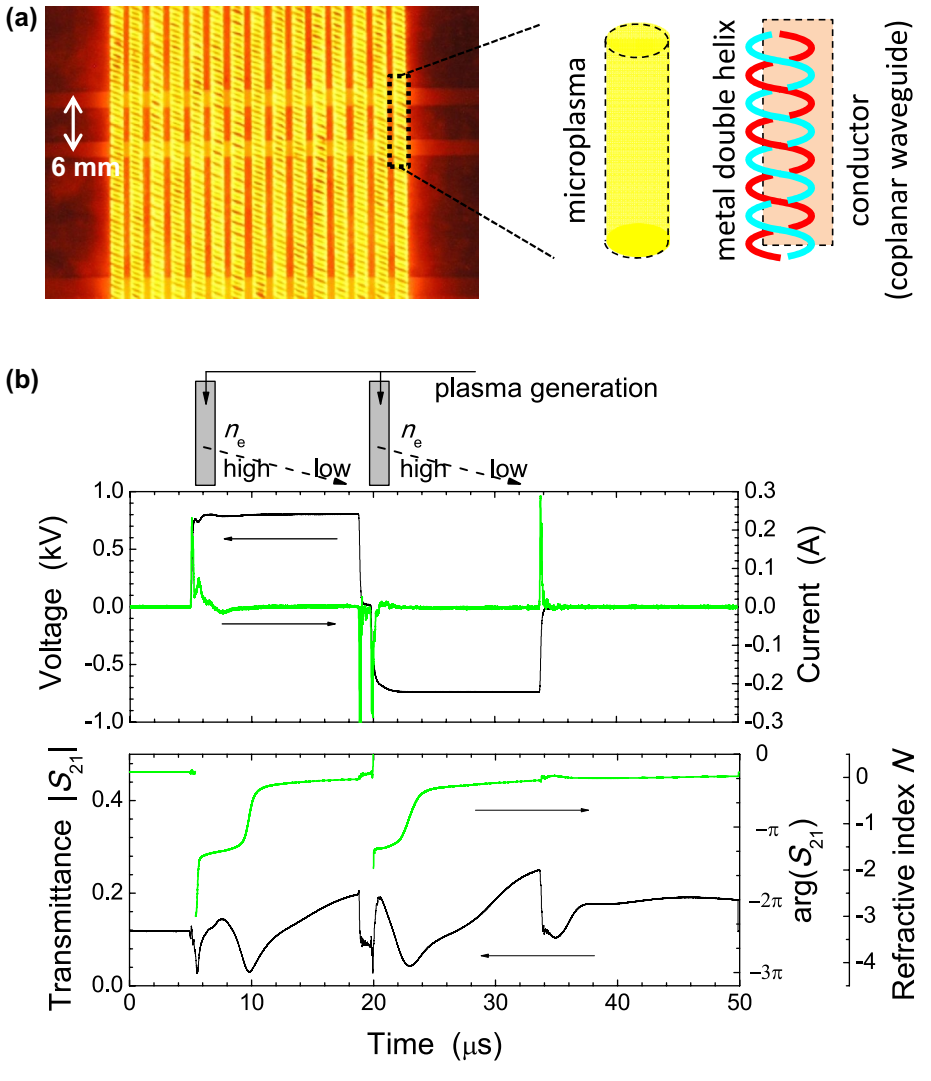


**Figure 4.** (a) Plasma-metamaterial composite on microwave coplanar waveguide, Ref. [14]. Emissions in yellow come from Ne plasma, and plasma is surrounded by metamaterial of double metal helices. (b) Time evolutions, Ref. [14], of discharge voltage and current, and amplitude and phase of transmitted wave with corresponding *N*.

Our experimental result shown here reconfirms that negative $\varepsilon$ is achievable by electron oscillations in discharge plasma at microwaves, which is not based on negative-$\varepsilon$ microwave metamaterials whose metallic components are assumed to be perfect conductors.

Different configurations of discrete structures of plasma and metamaterial were also investigated in other studies [38]. In all cases in Ref. [38], negative $N$ is expected, although their real and imaginary parts change the relative position between the microplasma and the $\mu$-controllable metamaterial in one meta-atom length.

### 3.2. Case of combined media with homogeneous material and discrete periodic microstructures

After confirmation of the validity of plasma in functions of metamaterials, synthesis of bulk and uniform plasma and discrete finite-size meta-atoms becomes a key issue. Plasma has a bulk property which is based on free electrons, with very small size, and it can also sneak into a metamaterial structure that has sufficient vacant space. Unlike metal materials, the imaginary part of $\varepsilon$ is controllable, and plasma can be a base (or background) medium that contains metamaterials. In these experiments, since the gas pressure was sufficiently low in comparison with the case of Figure 2, generated plasma was so diffusive that the profile of $n_e$ had almost no components of the spatial periodicity of DSRRs. Another fact different from the experiments shown in Subsection 3.1 is that direct measurements of $n_e$ is possible since the discharge space was sufficient for the probe diagnostics [39] that requires insertion of a small probe head (~ 1.0 mm) into the plasma region.

The experimental set-up was similar to the previous reports [30–32]. In brief, a negative-$\mu$ metamaterial was installed in a regular microwave rectangular waveguide at 2.45 GHz. Here, we use an array of DSRRs as negative-$\mu$ meta-atoms. One DSRR had a size of 9.2 mm with periodic length of 13 mm; both sizes are almost 1/10 of the wavelength at 2.45 GHz (~ 123 mm). Although DSRRs have metallic components parallel to $E$, their effects on $\varepsilon$ are so small that they cannot make $\varepsilon$ extraordinary, like making it negative [15,16]. To obtain collisionless plasma with negligible imaginary part of $\varepsilon$, the waveguide with the metamaterial was pumped into a vacuum with Ar gas at around 100 Pa. Then, a high-power pulsed microwave at 2.45 GHz with <500 W was launched at one end of the waveguide, and plasma was generated when the input power was beyond the threshold value (in tens of watts).

In advance of installation of the metamaterial, we monitored effective $\mu$ in a similar waveguide configuration by the parameter retrieval method [16], and calculated $\mu$ was −5.5−2.8j at 2.45 GHz, where the resonance frequency was at 2.39 GHz. Precisely, this value is valid when the metamaterial is in air or in low-pressure gas since equivalent capacitors in a DSRR have space for its gap on the pattern on a dielectric substrate. However, the frequency shift after plasma generation on its front is estimated as limited to 0.2 GHz [40], and the effective $\mu$ was still negative in our experimental condition.

When the plasma was generated, we monitored local values of $\varepsilon$ by the measurement of $n_e$ using a single Langmuir probe [30] since each space between DSRRs is sufficient (~ 10 mm) for both diffusive plasma generation and probe insertion. The probe measurement also suggests that electron temperature had values of 1–3 eV, which were typical values in this experimental condition. As a result, using the measured values of $\mu$ and $\varepsilon$, and assuming that $\mu$ is constant during plasma generation, we can derive $N$ via Equation (1) as shown in Figure 5 [31,32,41]. The values of $N$ indicate sufficiently large negative values after plasma generation; the

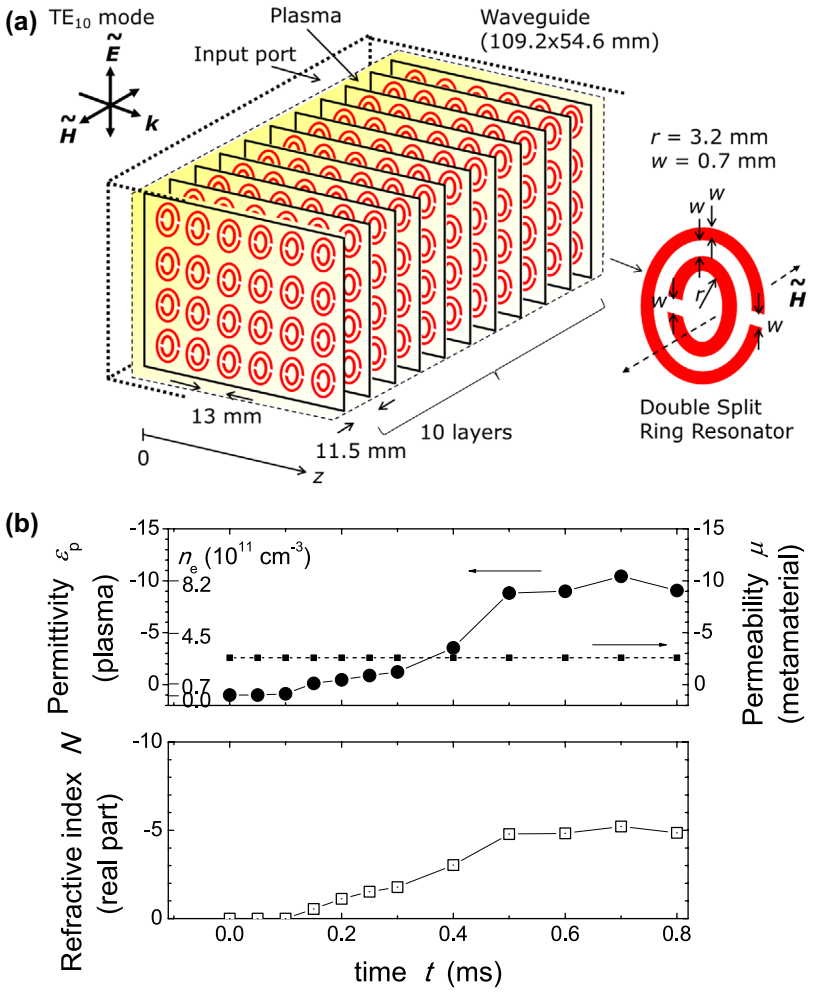


**Figure 5.** (a) Schematic view of plasma-metamaterial composite, Ref. [32]. (b) Time evolutions, Ref. [41], of $\varepsilon$, $\mu$, $n_e$ and $N$.

validity of these values is discussed later. Using data accumulated in experiments of different negative-$\mu$ metamaterials, we can make $\varepsilon$–$\mu$ and Re($N$)–Im($N$) diagrams, as shown in Figure 6. A close look at the data points in the $\varepsilon$–$\mu$ diagram reveal that there exists almost no point between 0 and +1 along the $\varepsilon$ axis (except one point derived from a transient built-up phase of plasma). This phenomenon is consistent with the theoretical prediction [14,31] in which the working point experiences a transition into the stable state with negative $\varepsilon$, whereas the region with positive $\varepsilon$ is unstable due to imaginary values of $N$. These experimental data suggest that the states of negative $N$ are successfully achieved.

The values of $N$ shown in Figures 5 and 6 are not obtained from diagnostics of propagating microwaves but calculated from Equation (1), and we have to confirm a possible propagating wave with estimated $N$. This further verification was performed by measurements of transmittance [30] and reflectance [32] of

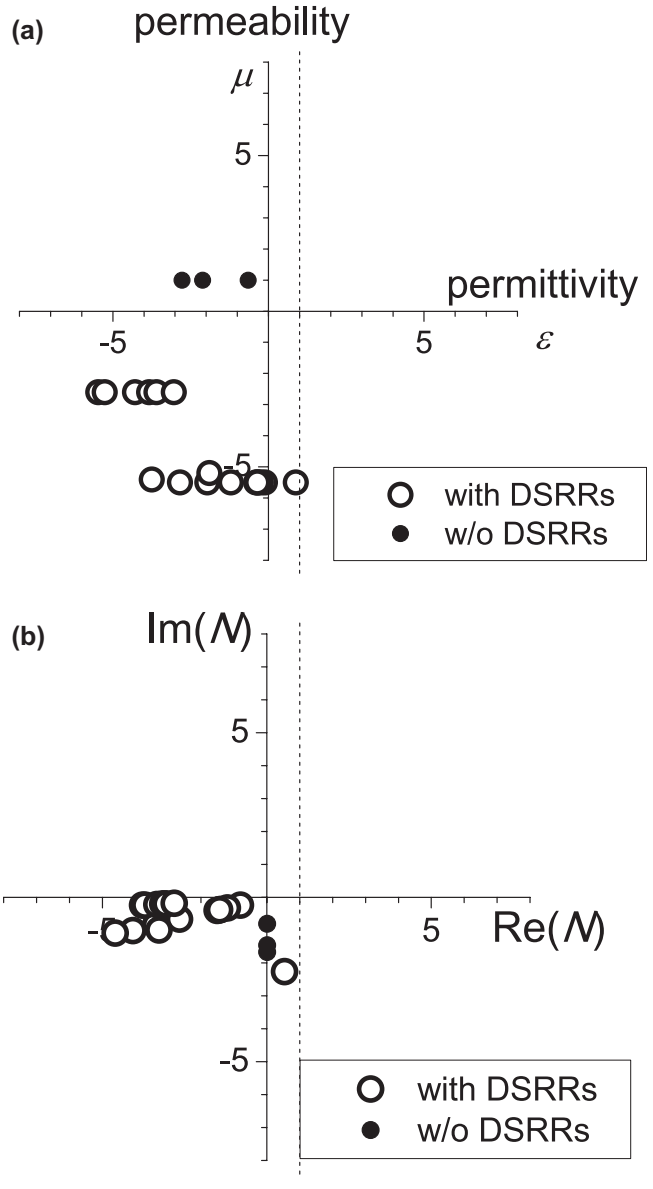


**Figure 6.** Diagrams of $\varepsilon$–$\mu$ and Re($N$) – Im($N$), Ref. [32], for various parameters in plasma-metamaterial composite.

propagating microwaves. One experimental confirmation of negative-$N$ states was based on enhanced transmitted waves in comparison with those in cases with imaginary $N$, i.e. with positive $\varepsilon$ and negative $\mu$ (before plasma generation in negative-$\mu$ metamaterial space) or with negative $\varepsilon$ and positive $\mu$ (high-density plasma generation in positive-$\mu$ space). We observed enhancement of transmitted waves [30] and also detected significant changes of phase in reflected waves; both of them can be understood only in the cases with a transition from positive- to negative-$\varepsilon$ states [32].

For the quantitative analysis, the estimated values of $N$ are compared with its range limited in the Bloch mode. Using the maximum value of $k$ in the spatial periodicity [42], $|N|$ in the Bloch mode is less than 4.7 through the term of $\pi c/a\omega$. This is in good agreement with the maximum value of $N$ ($\sim -5.0$) estimated from the values of $\varepsilon$ and $\mu$ in the experiments shown in Figures 5 and 6. Note that the plasma in this experimental setup was generated by propagating waves themselves, and this fact is consistent with the saturated time evolution of $N$ in Figure 5 for the following reason. As we noted, in an overdense plasma with negative $\varepsilon$ immersed in a negative-$\mu$ metamaterial, electromagnetic waves can propagate in the plasma-metamaterial composite. In our case, microwaves propagate inside the region, and they contribute to generating plasma or increasing $N$ with their energetic level, leading to further increase in $|\varepsilon|$. Then, after $N$ reaches the maximum value, wave propagation changes to *decrease* $N$ by an increment of $n_e$, with possible folded curves on the boundary of the first Brilluin zone. This underlying process causes the seeming saturation in Figures 5 and 6.

These results confirm achievements of negative-$N$ media using plasma-metamaterial composites whose $N$ is within the range of the Bloch mode depending on the periodic length of the meta-atoms. In such a composite, plasma is a kind of homogeneous medium or has a very small size of constituent particles (electrons), whereas metamaterials have a size around 1/10 of the wavelength.

## 4. Numerical analysis using various configurations

Since an experimental setup cannot achieve every possible configuration and parameter, we use a numerical method to investigate further details with various parameters to observe effects of meta-atom sizes in metamaterials. Here, we assume sets of hypothetical parameters that are general throughout metamaterials, not based on a specific configuration like a DSRR.

### 4.1. Numerical method

To see effects of free electrons in plasma, we perform one-dimensional particle simulations in which electrons and positive ions are mobile. The details of the numerical method are described in Ref. [43,44]. In brief, charge to mass ratio for electrons is $-1.0$, whereas that for positive ions is $10^{-4}$, and their density is the same, distributed uniformly from position $x = 12.8$–$25.6$. Setting the electron plasma frequency as 1.4142, the frequency of the incident wave is 1.0, which means that $\varepsilon = -1$ for the wave. Here, since motions of electrons are rigorously traced via motions of equations, we can observe wave propagation in a more realistic mode close to the experimental condition in comparison with finite-difference time-domain calculations in which $\varepsilon$ is given in a fluid assumption.

We also set the hypothetical magnetic resonance frequency, which is assumed to be $1 - \omega_m^2/\omega^2$ with $\omega_m = 1.4142$; $\mu$ is assumed to be in the Drude model in

which $\mu$ is negative when $\omega < \omega_m$ [45]. Consequently, $N$ is positive for $\omega > \omega_m$ and negative for $\omega < \omega_m$; in particular, $N = -1$ with $\omega = 1$, leading to a power matching condition on the interface. The width of this region is about 2 wavelengths, and it is not close to the infinite propagation, although we can obtain sufficient information for wave propagation.

### 4.2. Various configurations of discrete and/or homogeneous structures

To confirm reproducibility of experimental results, we calculate wave propagation in the plasma region with various sizes of the discrete units of the metamaterial with $\omega_m$. Within one discrete structure, we assumed *uniform* magnetic momentum caused by the magnetic resonance. Figure 7 shows three cases of one-dimensional wave propagation in time $t$. When the size of the unit is 1/5 of the wavelength $\lambda$, which may be the largest size of metamaterial units since the size of $(1/2)\lambda$ causes the first bandgap that is not an effect of metamaterials, we successfully observed negative phase velocity in the target region, with confirmation of negative $N$. However, the value of the averaged phase velocity in the target region, easily derived as a gradient of this diagram since the phase velocity is given by $x/t$, is larger than that in vacuum, by a factor of 1.23, leading to $N \sim -0.81$. This decrease might be attributable to the microscopic mismatching of phases (or inclusion of higher-order perturbation locally affecting the total phase information) between electric and magnetic fields. When the size is $(1/10)\lambda$, we observe almost ideal achievement of negative $N$ with slight decrease of $N$ ($\sim -0.93$). In the case with $(1/100)\lambda$, we observe a similar wave propagation to the case with synthesis of two homogeneous media for $\mu$ and $\varepsilon$. As a result, we can confirm good achievement of negative $N$ using homogeneous plasma and discrete metamaterial whose size is at least 10 times smaller than the wavelength.

To observe further variation of effects of the unit lengths in the unit for $\varepsilon$ (plasma in our case), we replace the plasma media with the Drude media in which $\varepsilon$ is as a function of $n_e$ that is set as a constant value in advance. Figure 8 shows one-dimensional wave propagation in time and the corresponding dispersion relation in the case of both discrete unit structures with $(1/10)\lambda$, where each structure is not synchronized but alternatively placed with the $(1/20)\lambda$ step. This case causes mismatching of the power transfer due to impedance gaps just on the interface, leading to significant reflected waves. However, the transmitted waves show negative phase velocity, similar to the case of Figure 7(b). This calculation result indicates that, synchronization of discrete structures of metamaterials not always being required, the synthesis effects are roughly possible after separate integration of contributions from $\mu$ and $\varepsilon$.

### 4.3. Discussion

The above numerical analysis confirms that $\varepsilon$ and $\mu$ can be estimated separately and then synthesized over one wavelength. In other words, even if the spatial

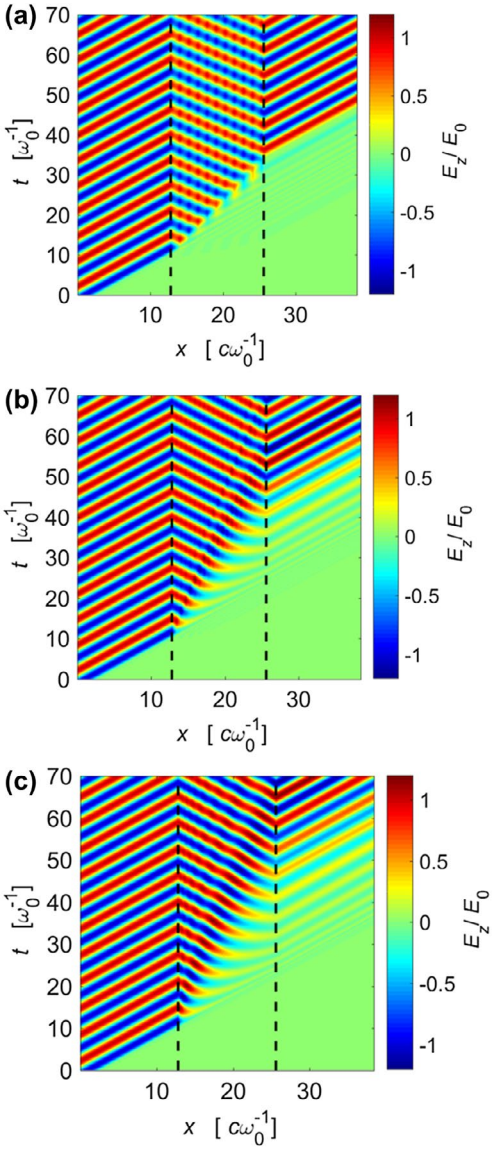


**Figure 7.** Numerical results on time evolutions of $E$ of propagating waves and dispersion relations in homogeneous plasma. (a) $E$ when size of meta-atoms for control of $\mu$ is $(1/5)\lambda$. (b) $E$ when meta-atom size is $(1/10)\lambda$. (c) $E$ when meta-atom size is $(1/100)\lambda$.

synchronization is not completed, the definition of metamaterials, implying that the unit size of their microstructure is almost equal to or less than $(1/10)\lambda$, assures that synthesis of two constituents for $\mu$ and $\varepsilon$ for electromagnetic metamaterials or for $M$ and $\rho_0$ for acoustic metamaterials are sufficient by estimations of separate integrations throughout a given space. Some studies [38] indicate that the values of $\varepsilon$ and $\mu$ depend on relative positions of elements in a unit structure. In such cases, two elements are frequently connected in one equivalent circuit. However, each element can be separated in an equivalent circuit, and similar underlying physics will be applicable.

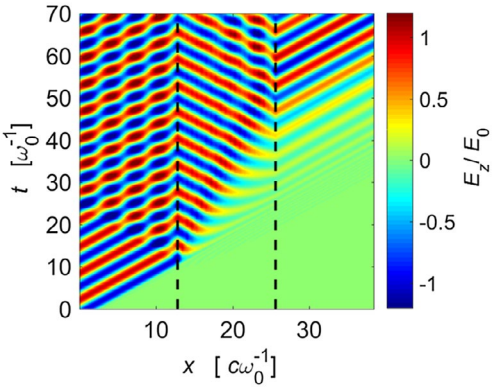


**Figure 8.** Numerical results on time evolutions of $E$ in propagating waves in case of discrete unit structures of both metamaterials for $\varepsilon$ and $\mu$ with length of $(1/10)\lambda$, where each structure is not synchronized but alternatively placed with the $(1/20)\lambda$ step.

The results discussed here are the cases where we can assume that spatial profiles of $\varepsilon$ and $\mu$ are *flat within one unit length*. Actually, following the experimental results in Section 3, homogeneous plasma and discrete metamaterials matched very well to create negative-$N$ material. However, the missing points of these experimental results are behaviors just around resonance points; the similar plot of process description is true at off-resonance frequencies in which negative $\mu$ is valid slightly apart from the resonance frequency.

Then, the remaining related issue is an effect of resonance properties themselves, where metamaterials usually include resonances to exhibit extraordinary values of $\varepsilon$ or $\mu$. One theoretical report on resonance and anti-resonance behaviors predicts that anti-resonance behaviors are unavoidable unless we use finite size of the unit structure, even if the size is very small in comparison with the wavelength [42]. In summary, we can confirm invariance of metamaterial parameters, given by Equations (1)–(3), on the unit size in various configurations, but there are still singular and irregular points as long as we use resonance features to obtain negative-$\mu$ states.

## 5. Concluding remarks and future perspectives

Metamaterials have properties like $N$ that arises from multi-constituents of unit microstructures, and their synthesis effects are almost always possible regardless of spatial synchronous configurations between the constituents. Experimental results reported so far verify that plasma, a homogeneous medium for negative-$\varepsilon$, and negative-$\mu$ metamaterial can be synthesized so well that $N$ becomes negative. Numerical analyses reconfirm this fact, and also indicate that various other combinations of the constituents with different spatial periodicities or with spatially unsynchronized pairs can create negative $N$ states. Although some remaining issues for specific resonance configurations are addressed, the conclusions here

can support more varieties of metamaterial designs with arbitrary periodic length of meta-atoms.

On the basis of this conclusion, we can approach a more flexible design of metamaterials. Meta-atoms so far have spatial periodicity in general. However, as explored in Ref. [28], rough spatial periodicity works well to exhibit extraordinary properties of metamaterials, which indicates that spatial integration to ensure effective and equivalent properties plays a crucial role. For an ultimate case, self-organized patterns with multi-scale periodicity like fractal structures [46–48] will be favorable for commercially available optical metamaterials.

Another point we stress here is the role of a homogeneous medium. Since a homogeneous medium and a discrete array of meta-atoms are well synthesized to create negative $N$, various possible configurations free from resonances and anti-resonances are worthwhile for future scientific targets. Because gaseous plasma has no substantial spatial periodicity and no limitation of $n_e$, $\varepsilon$ can be set free from restrictions that metamaterials have suffered thus far. There may be other materials that can work in a similar manner to a plasma; for instance, organic conductive materials or doped polymers show flexible $\varepsilon$ via photoinduced changes, being sufficiently homogeneous and free from rigorous spatial periodicity [49]. Such a material is suitable for potential optical metamaterials and installation for photonic devices. Thus, although these studies achieved using plasma at microwaves, common underlying physics will expand to acoustics and optics.

## Acknowledgements

One of the authors (OS) thanks Prof. S. Sakamoto at the University of Shiga Prefecture for discussion on acoustic metamaterials.

## Disclosure statement

No potential conflict of interest was reported by the authors.

## Funding

This study was supported by Grant-in-Aid for Scientific Research from the Japanese Ministry of Education, Culture, Sports, Science and Technology, Japan (JSPS KAKENHI [grant numbers JP22340171], [grant number JP26246035]).

## References

[1] A. Sihvola (ed.), *Advances in Electromagnetics of Complex Media and Metamaterials*, Kulwer Academic Publishers, Dordrecht, 2002.
[2] D.R. Smith, J.B. Pendry and M.C.K. Wiltshire, Science 305 (2004) p.788.
[3] C. Caloz and T. Itoh, *Electromagnetic Metamaterials: Transmission Line Theory and Microwave Applications*, Wiley-IEEE Press, Hoboken, 2006.
[4] N. Engheta, Science 317 (2007) p.1698.

[5] V.M. Shalaev, Nature Photo. 1 (2007) p.41.
[6] L. Solymar and E. Shamonina, *Waves in Metamaterials*, Oxford University Press, Oxford, 2009.
[7] C.M. Soukoulis and M. Wegener, Nature Photo. 5 (2011) p.523.
[8] M. Kadic, T. Buckmann, R. Schittny and M. Wegener, Rep. Prog. Phys. 76 (2013) p.126501.
[9] W. Rotman, IEEE Trans. Antennas Propag. 10 (1962) p.82.
[10] T.W. Ebbesen, H.J. Lezec, H.F. Ghaemi, T. Thio and P.A. Wolff, Nature 391 (1998) p.667.
[11] J.B. Pendry, A.J. Holden, D.J. Robbins, W.J. Stewart and I.E.E.E. Trans, IEEE Trans. Microw. Theory Tech. 47 (1999) p.2075.
[12] V.G. Veselago, Sov. Phys. Usp. 10 (1968) p.509.
[13] J.B. Pendry, L. Martin-Moreno and F.J. Garcia-Videl, Science 305 (2004) p.847.
[14] O. Sakai and K. Tachibana, Plasma Sources Sci. Technol. 21 (2012) p.013001.
[15] D.R. Smith, S. Schultz, P. Markos and C.M. Soukoulis, Phys. Rev. B 65 (2002) p.4773.
[16] D.R. Smith, D.C. Vier, T. Koschny and C.M. Soukoulis, Phys. Rev. E 71 (2005) p.377.
[17] D.K. Kalluri, *Electromagnetics of Complex Media*, CRC Press, Boca Raton, FL, 1998.
[18] S.H. Lee, C.M. Park, Y.M. Seo, Z.G. Wang and C.K. Kim, Phys. Rev. Lett. 104 (2010) p.054301.
[19] J. Li and C.T. Chan, Phys. Rev. E 70 (2004) p.055602(R).
[20] S.A. Cummer and D. Schurig, New J. Phys. 9 (2007) p.45.
[21] B.-I. Popa and S.A. Cummer, Phys. Rev. B 80 (2009) p.174303.
[22] S.H. Lee, C.M. Park, Y.M. Seo, Z.G. Wang and C.K. Kim, J. Phys. Condens. Matter 21 (2009) p.175704.
[23] R.A. Shelby, D.R. Smith and S. Schultz, Science 292 (2001) p.77.
[24] D.R. Smith, W.J. Padilla, D.C. Vier, S.C. Nemat-Nasser and S. Schultz, Phy. Rev. Lett. 84 (2000) p.4184.
[25] S. Zhang, W. Fan, N.C. Panoiu, K.J. Malloy, R.M. Osgood and S.R.J. Brueck, Phys. Rev. Lett. 95 (2005) p.1385.
[26] G. Dolling, C. Enkrich, M. Wegener, C.M. Soukoulis and S. Linden, Science 312 (2006) p.892.
[27] V.M. Shalaev, W. Cai, U. Chettiar, H.-K. Yuan, A.K. Sarychev, V.P. Drachev and A.V. Kildishev, Opt. Lett. 30 (2005) p.3356.
[28] T. Brunet, A. Merlin, B. Mascaro, K. Zimny, J. Leng, O. Poncelet, C. Aristegui and O. Mondain-Monval, Nature Mat. 14 (2014) p.384.
[29] O. Sakai, J. Maeda, T. Shimomura and K. Urabe, Phys. Plasmas 20 (2013) p.073506.
[30] O. Sakai, T. Naito and K. Tachibana, Plasma Fusion Res. 4 (2009) p.052.
[31] Y. Nakamura, A. Iwai and O. Sakai, Plasma Sources Sci. Technol. 23 (2014) p.064009.
[32] O. Sakai, Y. Nakamura, A. Iwai and S. Iio, Plasma Sources Sci. Technol. 25 (2016) p.055019.
[33] F. Forstmann and R.R. Gerhardts, *Metal Optics Near the Plasma Frequency*, Springer-Verlag, Berlin, 1986.
[34] K. Tachibana and I.E.E.J. Trans, Electr. Electron. Eng. 1 (2006) p.145.
[35] F. Iza, G.J. Kim, S.M. Lee, J.K. Lee, J.L. Walsh, Y.T. Zhang and M.G. Kong, Plasma Process. Polym. 5 (2008) p.322.
[36] O. Sakai, T. Shimomura and K. Tachibana, Phys. Plasmas 17 (2010) p.123504.
[37] S.S. Bedair, I. Wolff and I.E.E.E. Trans, IEEE Trans. Microw. Theory Tech. 40 (1992) p.41.
[38] K. Kourtzanidisa, D.M. Pederson and L.L. Raja, J. Appl. Phys. 119 (2016) p.204904.
[39] J.D. Swift and M.J.R. Schwar, *Electrical Probes for Plasma Diagnostics*, Iliffe, London, 1970.
[40] A. Iwai, Y. Nakamura, A. Bambina and O. Sakai, Appl. Phys. Express 8 (2015) p.056201.
[41] I. Adamovich, S.D. Baalrud, A. Bogaerts, P.J. Bruggeman, M. Cappelli, V. Colombo, U. Czarnetzki, U. Ebert, J.G. Eden, P. Favia, D.B. Graves, S. Hamaguchi, G. Hieftje, M. Hori, I.D. Kaganovich, U. Kortshagen, M.J. Kushner, N.J. Mason, S. Mazouffre,

S. Mededovic Thagard, H.-R. Metelmann, A. Mizuno, E. Moreau, A.B. Murphy, B.A. Niemira G.S. Oehrlein, Z.L. Petrovic, L.C. Pitchford, Y.-K. Pu, S. Rauf, O. Sakai, S. Samukawa, S. Starikovskaia, J. Tennyson, K. Terashima, M.M. Turner, M.C.M. van de Sanden and A. Vardelle, J. Phys. D: Appl. Phys. 50 (2017) p.323001.

[42] T. Koschny, P. Markoš, D.R. Smith and C.M. Soukoulis, Phys. Rev. E 68 (2003) p.056625.

[43] Y. Omura and H. Matsumoto, *KEMPO1: Technical guide to one-dimensional electromagnetic particle code*, in *Computer Space Plasma Physics: Simulation Techniques and Softwares*, H. Matsumoto and Y. Omura, eds., Terra Scientific, Tokyo, 1993, p. 21.

[44] A. Iwai, O. Sakai and Y. Omura, Phys. Plasmas 24 (2017) p.122112.

[45] R.W. Ziolkowski and E. Heyman, Phys. Rev. E 64 (2001) p.509.

[46] B.B. Mandelbrot, *The Fractal Geometry of Nature*, Freeman, San Fransisco, 1982.

[47] A.L. Barabasi and H.E. Stanley, *Fractal Concepts in Surface Growth*, Cambridge University Press, Cambridge, 1995.

[48] O. Sakai, Y. Hiraoka, N. Kihara, E. Blanquet, K. Urabe and M. Tanaka, Plasma Chem. Plasma Process. 36 (2016) p.281.

[49] H. Sakai, H. Murata, M. Murakami, K. Ohkubo and S. Fukuzumi, Appl. Phys. Lett. 95 (2009) p.252901.